Published in final edited form as:
Dev Neurobiol. 2008 February 1; 68(2): 166–181. doi:10.1002/dneu.20568.

Ganglion Cell Regeneration Following Whole-Retina Destruction in Zebrafish

Tshering Sherpa[1,2], **Shane M. Fimbel**[3], **Dianne E. Mallory**[1,2], **Hans Maaswinkel**[3], **Scott D. Spritzer**[1,2], **Jordan A. Sand**[1,2], **L. Li**[3], **David R. Hyde**[3], and **Deborah L. Stenkamp**[1,2]

1*Department of Biological Sciences, University of Idaho, Moscow, Idaho*

2*Neuroscience Graduate Program, University of Idaho, Moscow, Idaho*

3*Center for Zebrafish Research, University of Notre Dame, Notre Dame, Indiana*

Abstract

The retinas of adult teleost fish can regenerate neurons following injury. The current study provides the first documentation of functional whole retina regeneration in the zebrafish, *Danio rerio*, following intraocular injection of the cytotoxin, ouabain. Loss and replacement of laminated retinal tissue was monitored by analysis of cell death and cell proliferation, and by analysis of retina-specific gene expression patterns. The spatiotemporal process of retinal ganglion cell (RGC) regeneration was followed through the use of selective markers, and was found to largely recapitulate the spatiotemporal process of embryonic ganglion cell neurogenesis, over a more protracted time frame. However, the re-expression of some ganglion cell markers was not observed. The growth and pathfinding of ganglion cell axons was evaluated by measurement of the optic nerve head (ONH), and the restoration of normal ONH size was found to correspond to the time of recovery of two visually-mediated behaviors. However, some abnormalities were noted, including overproduction of RGCs, and progressive and excessive growth of the ONH at longer recovery times. This model system for whole-retina regeneration has provided an informative view of the regenerative process.

Keywords

retinal ganglion cell; retina; regeneration; Zebrafish; gene expression

INTRODUCTION

In mammals including humans, retinal injuries and retinal diseases result in the irreversible loss of retinal neurons, leading to blindness. The retinas of teleost fish, in contrast, possess the intrinsic capacity to replace cells that were lost to chemical, thermal, light, or mechanical damage (Lombardo, 1972; Maier and Wolburg, 1979; Raymond et al., 1988; Hitchcock et al., 1992; Braisted et al., 1994; Cameron, 2000; Vihtelic and Hyde, 2000; Fimbel et al., 2007). This capacity is likely related to the ability of the fish retina to continue to generate new retinal neurons throughout life, a process referred to as persistent neurogenesis (Stenkamp, 2007; Hitchcock et al., 2004). One of the modes of persistent neurogenesis is the ongoing addition of new retinal neurons at the retinal margin, from a proliferative neuroepithelial tissue called the circumferential germinal zone (CGZ; Raymond and Easter, 1983). The second mode is the production of rod photoreceptors from a defined lineage of progenitors. The stem cells of this

Correspondence to: D.L. Stenkamp (dstenkam@uidaho.edu).

Published online 13 November 2007 in Wiley InterScience (www.interscience.wiley.com).

lineage, recently identified as Müller glia (Bernardos et al., 2007), reside in the inner nuclear layer (INL) and generate proliferative progeny that migrate to the outer nuclear layer (ONL) (Raymond, 1985; Julian et al., 1998; Marcus et al., 1999; Otteson et al., 2001). The proliferative cells of the ONL are called rod precursors, and are the most immediate source of new rod photoreceptors (Johns and Fernald, 1981; Raymond and Rivlin, 1987). Following injury, Müller glia proliferate, and the fates of their progeny are altered to generate all classes of retinal neurons (Wu et al., 2001; Yurco and Cameron, 2005; Bernardos et al., 2007; Fausett and Goldman, 2006; Fimbel et al., 2007; Kassen et al., in press). The process of regeneration takes place essentially as an injury-induced recapitulation of retinal development, as many of the genes involved in retinal development are re-expressed during regeneration (Hitchcock et al., 2004).

The regenerative process in teleost retina has inspired the search for similar, though latent mechanisms in the retinas of other taxa, which may be manipulated so as to promote retinal regeneration. For example, the chicken retina can respond to injury by generating some new retinal neurons (Fischer and Reh, 2001), and there is now sufficient evidence that stem cells capable of generating new neurons are present in the mammalian retina (Ahmad et al., 2000; Tropepe et al., 2000). These findings lend support for the development of treatments for human retinal disease that recruit or transplant these cells to regenerate missing or damaged neurons. However, in order for these treatments to be successful, the new neurons must develop in a manner so as to establish the appropriate connections and so as to be functional. Regenerated retinal ganglion cells (RGCs) in particular must meet the challenge of producing axons that successfully navigate to the optic nerve head (ONH) and to appropriate targets in the brain. Furthermore, the entire process must take place in an environment that has been adversely affected by the underlying pathology of the retinal disease or injury.

In this study, we wish to establish not only the capacities, but also the potential limitations of RGC regeneration, in a model that permits current and future use of genetic resources: the zebrafish. We use intraocular injections of the Na+/K+ ATPase inhibitor ouabain to destroy all retinal neurons and initiate a regenerative response (Maier and Wolburg, 1979; Raymond et al., 1988; Mensinger and Powers, 1999; Stenkamp et al., 2001; Fimbel et al., 2007). This method was selected for two reasons. First, complete destruction of the retina permits the evaluation of the loss and re-establishment of visual function through the monitoring of visually-mediated behaviors (Kästner and Wolburg, 1982; Li and Dowling, 1997; Mensinger and Powers, 1999). Second, any application of regenerative therapy in the case of a human disorder will need to take place amid underlying retinal pathology; the intraocular ouabain treatment, while not precisely mimicking any specific human disorder, does generate a pathological environment (Wolburg, 1975; Raymond et al., 1988) that may similarly challenge the regenerative process. Following this treatment, we monitored the regenerative response histologically, behaviorally, and genetically, with a focus on the regeneration of RGCs. Three hypotheses tested were as follows: (1) Zebrafish, like goldfish, can functionally regenerate retina following whole-retina destruction with a cytotoxin (Kästner and Wolburg, 1982; Mensinger and Powers, 1999), and can therefore serve as a model system for understanding whole-tissue retinal regeneration. (2) Because the spatiotemporal expression pattern of individual genes during regeneration resembles that observed during embryonic retinogenesis (Levine et al., 1994; Hitchcock et al., 1996; Sullivan et al., 1997; Liu et al., 2002; Fimbel et al., 2007), we hypothesized that the relative spatiotemporal patterns of multiple genes involved in RGC development would be recapitulated during RGC regeneration, implying that regenerating RGCs develop as they do during embryogenesis, in a manner consistent with the restoration of visual function. (3) In the course of our experiments we found a considerable temporal delay between histological regeneration of retinal tissue and behavioral recovery of visual function, and therefore hypothesized that a limiting factor for functional retinal regeneration following whole-tissue injury is the navigation of RGC axons to their targets. A

corollary of this latter hypothesis is that the size of the ONH, containing regenerating RGC axons, will predict loss and recovery of visual function. Therefore, we measured ONH diameters, and tested visual function recovery using two behavioral assays, in ouabain-treated zebrafish.

METHODS

Animals and Intraocular Injections

Animals—Adult (3–12 month) zebrafish of a mature size (3 cm total body length) were either of the AB strain, or of a strain originally purchased from Scientific Hatcheries (Huntington Beach, CA), and were maintained and bred in-house according to Westerfield (2000), in monitored aquatic housing units on recirculating water system. Fish rooms were on an L/D cycle of 14:10 h, at 28.5°C. All procedures were approved by the Animal Care and Use Committees of the University of Idaho and the University of Notre Dame, and conformed to the ARVO Statement on Animal Research.

Ouabain Injections—Experimental fish were anaesthetized in buffered tricaine methanesulphonate (MS-222; Sigma, St. Louis, MO) (Westerfield, 2000), or a 1:1000 dilution of 2-phenoxyethanol, and a microscalpel was used to make a small incision through the cornea and iris in the ventronasal quadrant of the right eye. A blunt-end 33-gauge Hamilton syringe (Hamilton, Reno, NV) was introduced into this incision with the aid of a micromanipulator (Narishige, Japan), and 0.5 μL of 200 μM ouabain (Sigma) in sterile 0.9% saline was injected into the space behind the lens. This amount was estimated to result in an intraocular concentration of 10 μM, based on calculations derived from the geometry and volumes of the eye and lens (Raymond et al., 1988). With the exception of the escape response assay (see later), left (control) eyes were either not injected, or were injected with an equivalent volume of 0.9% sterile saline. Fish were allowed to recover in water system before being returned to the fish facility.

Escape Response—The behavioral escape response test was used to evaluate visual threshold (Li and Dowling, 1997). The test apparatus consisted of a circular transparent plastic container (inner diameter, 112 mm) surrounded by a drum (inner diameter, 152 mm), turning at 10 rotations per minute in either a clockwise or counterclockwise direction. The inside of the drum was covered by white paper and marked with a black segment (64 mm wide). The drum was illuminated from above with white light, maximum intensity, 425 $\mu W/cm^2$ (log [I] = 0). The intensity of the light source was adjusted by adding or removing neutral density filters. An infrared camera was suspended above the drum to record the escape response of individual fish.

Following bilateral retinal injection with a final intravitreal concentration of either 10 μM ouabain (n = 8) or 0.65% saline (n = 10), fish were placed in individually numbered tanks. During testing, the experimenter was unaware of each animal's treatment, and on each testing day, the sequence of testing was randomized among the test fishes. Before testing, each fish was habituated for at least 30 min in the dark experimental room before testing the escape responses to a rotating black stripe. At the start of the test, the light intensity was set at log [I] = −6.0 and was incrementally (in 0.5 log increments) increased until the fish reacted with at least five responses in 10 encounters. A positive escape response consisted of either (a) a 180° reversal of swimming direction, or (b) a redirection toward the center of the drum followed by resuming swimming near the drum wall after they passed the black segment (Li and Dowling, 1997). The light intensity was noted as the visual threshold. The testing was performed between 2 and 6 P.M., the time of day when the fish are most sensitive to light (Li and Dowling, 1998). Statistical analyses were performed using SPSS 11.0.4 for Mac OS X.

Dorsal Light Reflex—A total of 38 experimental fish were monitored daily for evidence of an abnormal dorsal light reflex (DLR). The DLR allows fish to maintain body axis orientation in the water column, using downwelling light as the environmental cue (Silver, 1974). Damage to a single eye, resulting in unilateral loss of visual function, causes a fish to tilt such that the damaged eye looks upward toward the source of downwelling light (Mensinger and Powers, 1999). The DLR was assessed by three independent, naïve observers; a definitive DLR score (normal vs. abnormal) was noted only if all observers agreed on this score. Fish that did not show an abnormal DLR (body tilt) within 24 h of ouabain treatment, were not considered further.

BrdU Treatments—For some experiments, 5 days after ouabain injection, fish were transferred to beakers containing 5 m*M* bromodeoxyuridine (BrdU; Sigma) in system water, where they were maintained for 48 h. These fish were then transferred to beakers containing unmodified system water for 2 h prior to being returned to the fish facility.

Histological Methods

At selected times after ouabain treatment, fish were anaesthetized, their spinal cords were transected and eyes were removed. Corneas were perforated, and the lenses were removed. During these procedures, gross anatomical characteristics of the eye were noted, including pupil shape and size, optic nerve color and integrity, lens characteristics, and general eye morphology.

Retinal Whole Mounts—Retinas were removed from the eyes as whole mounts and were placed in 4% paraformaldehyde in buffered 5% sucrose for 1 h. Retinas were washed in buffered 5% sucrose then stored at −20°C in 100% MeOH.

Retinal Cryosections—For some procedures (*in situ* hybridization, and immuncytochemistry other than that for proliferating cell nuclear antigen; PCNA), tissue was processed according to Barthel and Raymond (1990). Whole eyes were placed in 4% paraformaldehyde in buffered 5% sucrose for 1 h. Eyes were washed in buffered 5% sucrose, and then in increasing concentrations of sucrose before cryoprotection overnight at 4°C in buffered 20% sucrose. Eyes were embedded in a solution of 1 part OCT embedding medium (Sakura Finetek, Torrance, CA) and 2 parts buffered 20% sucrose and sectioned at 5 μm on a cryostat. For PCNA immunocytochemistry, enucleated eyes were fixed overnight at 4°C in 9:1 ethanolic formaldehyde (95% ethanol:37% formaldehyde) (Vihtelic and Hyde, 2000). Fixed retinas were rehydrated through an ethanol series and cryoprotected in 30% sucrose/PBS (pH 7.4) for 4 h at room temperature or overnight at 4°C. Tissues were embedded in a 1:1 mixture of PBS:Tissue Freezing Medium (TFM; Triangle Biomedical Science; Durham, NC) containing 30% sucrose overnight at 4°C, and then were frozen for sectioning at 14 μm.

For all analyses, only central retinal regions were considered, to ensure that regeneration, rather than enhanced growth at the retinal margin (Raymond et al., 1988; Stenkamp et al., 2001), was being monitored.

Measurement of ONHs—Two distinct tissue-processing methods were used to obtain material for the measurement of the optic nerve heads (ONHs). The first method utilized cryosections according to the procedure of Barthel and Raymond (1990). Radially-oriented sections passing through the ONH were then stained with thionin (Eichler and Taylor, 1976), mounted in glycerol for brightfield microscopy on a Leica DMR microscope. For the second method, eyes were fixed in 2% formaldehyde/2.5% glutaraldehyde/100 m*M* Na cacodylate (pH 7.4) overnight at 4°C, and were then washed in 100 m*M* Na cacodylate for 30 min at room temperature. Tissue was dehydrated in ethanol, placed in 1:1 xylene/ethanol and 100% xylene/

Polybed 812, and finally into fresh Polybed 812 (Polysciences, Warrington, PA). This resin was polymerized at 60°C. Serial sections of 3 μm were cut along the dorsal–ventral axis using a glass knife on a JB4 microtome, and were stained with a 1:1 mixture of 1% methylene blue/1% azure II. There were no significant differences in ONH measurements from control eyes following these two different histological processing methods (data not shown). Images were collected using a SPOT camera and software (Diagnostic Instruments, Sterling Heights, MI) and imported into Scion Image software. For each section evaluated, three linear measurements of ONH diameter were obtained and averaged. Of these average measurements, only the highest value for each eye was considered as representing the diameter of the ONH (smaller values were interpreted as indicating that the section was not cleanly bisecting the ONH). Only ONHs with axons visibly passing from inside the eye to outside the eye were measured; those not meeting this criterion were assigned a diameter of zero.

Immunocytochemistry

Sections were blocked in 20% goat serum, and then one of the following monoclonal antibodies was used: zn8 (1:25), zn12 (1:500), and anti-Hu (1:200) were from the Zebrafish International Resource Center (University of Oregon, Eugene, OR); anti-islet-1 (1:200) was from the University of Iowa monoclonal stock center (Ames, IA); rat anti-BrdU (1:20) was purchased from Chemicon (Temecula, CA), mouse antiPCNA (clone PC10; 1:1000) was purchased from Sigma. Tissue was incubated with primary antibody overnight at 4°C. Sections were washed in phosphate buffered saline containing 0.5% Triton X-100 (PBST), then incubated for 2 h at room temperature with a 1:200 dilution of a Cy3-conjugated secondary antibody (Jackson Immunoresearch, West Grove, PA), or a 1:500 dilution of Alexa-Fluor 488-conjugated secondary antibody. Tissue was then washed, mounted in either Vectashield (Vector Laboratories, Burlingame, CA) or Prolong Gold (Molecular Probes, Invitrogen, Carlsbad, CA) antifade medium, and viewed under epifluorescence and Nomarski optics.

Whole mounted retinas were processed for islet-1 immunocytochemistry using a similar procedure, except tissue was incubated with secondary antibody overnight at 4°C. Whole retinas were mounted ganglion cell-side up in Vectashield, and viewed under epifluorescence optics on a Leica DMR compound microscope. At least two representative images from each processed retina were collected with a SPOT camera and software, and labeled cells were counted within a field of view (200 μm × 300 μm). Densities were calculated as numbers of labeled cells per mm^2.

Sections processed for PCNA immunocytochemistry were viewed on a Leica TCS SP5 Broadband Confocal System (Leica Microsystems GmbH). From each of six eyes, at least three sections from the central retina were selected for quantification. All PCNA-positive cells across the retina (with the exception of the region within 100 μm of the CGZ) on in-focus, single plane optical sections (focal depth 5 μm) were counted, and used to determine the average number of labeled nuclei per retina per time point. From each eye examined, at least two sections that included, or were adjacent to, the optic nerve were quantified.

Terminal dUTP Nick-End Labeling

Analysis of cell death following intraocular injection of ouabain was performed as described by Vihtelic and Hyde (2000). In brief, eyes were fixed in 3.7% formaldehyde/PBS for 4 h at room temperature, tissue was washed in PBS, and cryoprotected in 30% sucrose/PBS (pH 7.4) overnight at 4°C. Tissues were incubated in a 1:1 mixture of 30% sucrose/PBS:TFM overnight at 4°C and were embedded and frozen in 100% TFM. Sections were cut at 10 μm thickness on the dorsal-ventral axis. Apoptotic cells were labeled in cryosections using the TdT-mediated incorporation of streptavidin–fluorescein labeled dNTP (TACS TdT Kit; R&D Systems; Minneapolis, MN), according to the manufacturer's instructions. To enhance labeling, sections

were permeabilized with Neuropore (R&D Systems) for 75 min. Immediately following terminal dUTP nick-end labeling (TUNEL) labeling, tissue was mounted using Vectashield and viewed on a Leica TCS SP5 Broadband Confocal microscope (Leica Microsystems GmbH).

TUNEL-labeled nuclei were counted in three representative sections for each of six retinas sectioned at each time point; counts were segregated according to laminar position within the retina. All TUNEL-positive cells across the entire retina were counted on in-focus, single plane optical sections (focal depth 5 μm) and used to determine the average number of labeled nuclei per retina. These counts excluded both the dorsal and ventral margins (first 100 μm of tissue from the dorsal/ventral margin towards the optic nerve). Positive and negative controls included adding TACS-nuclease and omitting the TdT enzyme, respectively.

In situ Hybridization

Plasmids containing cDNAs for zebrafish *ath5*, *pax6*, and *fgf8* were the kind gifts of Steve Wilson (King's College, London); plasmid containing zebrafish *brn3b* cDNA was the kind gift of Jim Fadool (Florida State University). Digoxigenin-labeled (dig-) cRNA probes were prepared according to the Genius Users' Guide (Roche, Indianapolis, IN). *In situ* hybridizations were performed according to Barthel and Raymond (1993). Sections (or wholemounts) were rehydrated and incubated with 10 μg/mL proteinase K at 37°C, dehydrated, and then incubated with 1 mg/mL probe in a 50% formamide hybridization solution at 56°C. Hybridization was detected by using an anti-dig antibody conjugated to alkaline phosphatase (Roche) and the color substrates 4-nitroblue tetrazolium chloride and 5-bromo-4-chloro-3-indolyl phosphate (NBT/BCIP).

RESULTS

Cell Death and Cell Proliferation Following Intraocular 10 *μM* Ouabain

Intraocular injection of 10 μM ouabain results in loss of cells in all retinal layers, based upon histological analysis (Fimbel et al., 2007). To confirm that this treatment generated widespread retinal cell death, eyes of ouabain-treated fish were processed at 1, 2, 3, 4, and 5 days after injection for TUNEL analysis [Fig. 1(A–D)]. Cell death within the INLs was highest at 1, 2, and 3 days postinjection (dpi), while cell death in the ONL peaked at 3 dpi. Some residual apoptosis persisted in both layers through the last time point analyzed, 5 dpi. These results indicate that the 10 μM intraocular injection of ouabain was sufficient to cause widespread damage in all retinal cell layers, and that much of the damage was completed by 3 dpi.

To evaluate the proliferative response to retinal damage, eyes of ouabain-treated fish were processed at 3, 7, 10, 14, and 42 dpi for PCNA immunocytochemistry [Fig. 1(E–H)]. Cell proliferation, as measured by numbers of PCNA-positive cells, peaked at 7 dpi, but high numbers of PCNA-labeled cells persisted through 14 dpi, suggesting that the proliferative response to damage continues. The number of PCNA-positive cells observed at 42 dpi was greatly reduced relative to the earlier time points, but was still higher than the baseline number in control retinas. At 7 dpi, the distribution of PCNA-labeled cells was in most cases uniform across the regenerating retina, while at later times the distribution showed some patchiness [Fig. 1(F,G)].

To verify that proliferative cells were generating new cells, in all retinal layers, six fish were treated with ouabain, and then were systemically exposed to 5 m*M* BrdU on days five and six following injection. Two each of these fish were sacrificed 12, 15, and 20 days after the injection. BrdU labeling was seen in all layers of the retinas of these fish [Fig. 1(I–L)], indicating that retinal tissue was generated during the BrdU immersion—after the ouabain

injection—and constituted regenerated retina. In addition, retinas processed at 12 days after ouabain treatment consistently showed more extensive BrdU incorporation than those processed at later time points. Together with the PCNA data described earlier, this finding suggests that an initial burst of proliferative activity is followed by additional production of retinal cells during a time after the BrdU exposure.

Gross Anatomy of the Eye During Retinal Regeneration

Previous work in the goldfish has demonstrated that gross abnormalities of the eye accompany the regenerative process (Raymond et al., 1988; Mensinger and Powers, 1999); typical abnormalities include reduced pupil size due to iris overgrowth, and lens abnormalities such as opacities or lens duplications. Similarly, we noted the occurrence of several gross anatomical abnormalities in our ouabain-treated eyes (Table 1). Of greatest interest, iris/pupil abnormalities and lens abnormalities both appeared to increase in frequency with time following ouabain treatment, as would be expected if they were correlated with the regenerative state of the retina. However, abnormal eye morphologies were observed in approximately half of all experimental fish at each time point.

Does Ouabain-Induced Regeneration of RGCs Recapitulate the Genetic Cascade of RGC Neurogenesis Found During Development?

Retinal sections obtained from treated eyes and the untreated, contralateral control eyes were processed for *in situ* hybridization and indirect immunofluorescence with several ganglion cell markers. The spatiotemporal patterns of expression of these markers are summarized below and in Figures 2 and 3, and in Table 2.

The *ath5* gene is required for RGC neurogenesis in the zebrafish (Kay et al., 2001) and is the earliest known marker for the process of retinal neurogenesis in general (Masai et al., 2000). During retinal regeneration, *ath5* mRNA expression was observed in all experimental eyes examined at the earliest analysis time, 6 dpi [Fig. 2(A); Table 2]. This gene was expressed in clusters of retinal tissue having a neuroepithelial appearance, but expression was generally not retina-spanning (i.e., expressed by some progenitor cells but not all). Expression of *ath5* persisted in 60% of the eyes evaluated at 8 dpi [Fig. 2(E); Table 2], but expression was not seen in experimental eyes at later time points, nor in any of the control eyes (Table 2, and data not shown), indicating that *ath5* is expressed early, and transiently, during retinal regeneration.

In teleost fish, *pax6* is expressed in retinal progenitors during embryonic retinal development (Nornes et al., 1998), and later becomes restricted to RGCs and amacrine cells [Hitchcock et al., 1996; Fig. 2(R)], and to putative stem cells of the rod photoreceptor lineage (Otteson et al., 2001). Like *ath5*, *pax6* mRNA expression was also observed in all experimental eyes examined at 6 days after ouabain treatment [Fig. 2(B); Table 2], and the pattern of expression was retina-spanning, consistent with the patterns seen in embryonic retinal neuroepithelial tissue (Puschel et al., 1992). In experimental eyes obtained at 8 days following ouabain treatment, the pattern of *pax6* became more restricted, with reduced labeling in the apical regions of the regenerative clusters, coincident with the initial formation of retinal layers [Fig. 2(F); Table 2]. At 12 days following injection and later, the *pax6* labeling pattern resembled that of control retinas, with expression in the RGC layer and in the inner half of the INL [Fig. 2(J,N,R)]. *Pax6* was also expressed by cells residing ectopically in the inner plexiform layer [Fig. 2(J,N)]. These ectopic cells have been referred to as “laminar fusions” in goldfish models of retinal regeneration (Raymond et al., 1988; Hitchcock et al., 1992).

Islet-1 is a Lim-homeobox transcription factor expressed during RGC neurogenesis, and in RGCs and amacrine cells (Galli-Resta et al., 1997; Korzh et al., 1998). Islet-1-positive cells were found in all regenerating retinas at all time points examined [Fig. 2(C,D,K,O); Table 2].

Even at 6 and 8 dpi, some islet-1-labeled cells were present in the most vitread regions of the regenerating clusters [Fig. 2(C,D)]. Experimental eyes processed at later times contained islet-1-positive cells in the regenerated ganglion and amacrine cell layers [Fig. 2(K,O)], similar to the pattern in undamaged retina [Fig. 2(S)].

The Hu C/D antigen is an RNA binding protein present exclusively in neurons, and anti-Hu antibodies allow detection of newly-generated neurons in zebrafish (Kim et al., 1996). Hu-positive cells were found in regenerating retinas at all time points examined [Fig. 2(I,M), Table 2], as well as in undamaged retinas [Fig. 2(Q)].

Zn-8 (zn-5) is a monoclonal antibody that labels neurolin (DM-GRASP), a cell adhesion molecule on RGCs and their axons (Fashena and Westerfield, 1999). During teleost embryonic development, it is expressed most strongly during the time of axon outgrowth toward the tectum (Laessing and Stuermer, 1996; Ott et al., 2001). Zn-8-positive cells could not be found in retinas obtained at 6 dpi, and were present in three of five retinas examined at 8 dpi [Fig. 2(G,H); Table 2]. However, all retinas obtained 12 and 20 dpi demonstrated robust labeling [Fig. 2(L); Table 2]. The expression of neurolin was then down-regulated in some cases, as only two of five retinas obtained 70–90 days after ouabain injection showed zn-8 labeling [Fig. 2(P); Table 2]. Undamaged control retinas displayed very weak or no zn-8 labeling [Fig. 2(T); Table 2].

In retinas processed at the later survival times, we noted that the inner retina continued to change, with multiple layers of cells within as well as vitread to the inner plexiform layer; these cells could be labeled by RGC markers such as Hu C/D and islet-1 [Fig. 2(M–P)]. In contrast, undamaged control retinas showed a single layer of cells in the RGC layer with little or no invasion of cells into the inner plexiform layer [Fig. 2(Q–T)]. In the interests of further assessing any differences in RGC density, we processed three regenerated, and two control retinas for whole mount immunocytochemistry with the islet-1 antibody, using material obtained at time points beyond 100 days following ouabain injection. The density of islet-1-positive cells was higher in the regenerated samples than in the controls [Fig. 3(A–C)], consistent with overproduction of inner retinal cell types, including RGCs, following injury. We note that these cell density data represent only optically coplanar subsets of islet-1-positive cells, and therefore provide an underestimation of actual cell density, especially for regenerated retina, where islet-1-labeled cells clearly accumulated in a nonplanar arrangement. This pattern of cell accumulation precluded a complete comparative analysis of ganglion cell pattern in regenerated retina, as the methods available analyze two-dimensional patterns only (Stenkamp et al., 2001).

Several additional RGC markers were used to evaluate RGC regeneration, but clear interpretation of these labeling experiments was not possible. cRNA probes corresponding to zebrafish *Brn3b* (DeCarvalho et al., 2004), *fgf8* (Martinez-Morales et al., 2005), and *shh* (Neumann and Nuesslein-Volhard, 2000) did not generate any positive signals on adult retinal tissue, whether regenerating or undamaged control, either in whole mounts or on retinal cryosections. These probes, however, labeled newly-generated RGCs in whole-mounted zebrafish embryos [data not shown, see Neumann and Nuesslein-Volhard (2000); Stenkamp and Frey (2003); DeCarvalho et al., (2004)], suggesting that these markers may not be re-expressed during regeneration at levels sufficient for detection by *in situ* hybridization. The zn-12 antibody, which labels the HNK-1 epitope on neuronal cells and has been used to identify newly-differentiated neurons in the zebrafish (Hu and Easter, 1999), was also applied to retinal tissue, but this antibody very strongly labeled what appeared to be debris within the damaged eyes at the earlier survival times (data not shown), and we were not confident that we could reliably identify labeled neurons in these experiments.

Regeneration of the Optic Nerve Head

Radial sections of the retina containing the optic nerve head (ONH) were stained with either thionin or methylene blue/azure II, and images of these sections were imported into ScionImage for measurement of ONH diameter (see Methods). Diameters of ONHs from 14 undamaged control eyes were 164.4 ± 16.7 μm [Figs. 4(A) and 5]. At the earliest survival times following ouabain injection (1 and 4 dpi), the ONH remained recognizable, but became visibly smaller as the surrounding retinal tissue degenerated [Figs. 4(B) and 5]. In tissue obtained at 6, 7, 8, and 12 dpi, identification of the ONH was challenging, and in many cases probable ONHs contained no visible axons [Fig. 4(C)], or an exterior optic nerve stump was discontinuous with the interior of the eye and appeared to be barricaded with pigmented material [Fig. 4(D)]. These cases were assigned an ONH diameter of zero [Fig. 5]. At survival times of 20, 40, 85, and 120 days following ouabain injection, the ONHs were recognizable and contained passing axons. The diameters of these ONHs became progressively larger to match or exceed those of the control eyes [Figs. 4(E,F,G) and 6]. At survival times beyond 100 dpi, this growth continued, with two retinas containing ONHs nearly twice the diameter of control ONHs [Figs. 4(H) and 5].

Functional Regeneration

We used the escape response (Li and Dowling, 1997), as a behavioral assay to determine loss and recovery of visual function of adult zebrafish following the intraocular injection of 10 μM ouabain. The results of this assay, along with the subsequent statistical analysis, are presented in Figure 6. In these experiments, fish were subjected to intraocular injection of ouabain (experimental) or saline (control) in both eyes. At various times after the ouabain injection, between 1 and 182 dpi, the fish were individually exposed to a rotating stripe (predator) outside a circular tank. The ambient light intensity was modified until the fish successfully avoided the stripe on at least 5 out of 10 encounters. The minimal light intensity to produce this successful avoidance response was then recorded. Some fish did not survive the entire time-course of the experiment, with a total loss of three fish from the control group (n = 10 initially, and n = 7 at 182 days), and a loss of three fish from the ouabain group (n = 8 initially, and n = 5 at 182 days).

These data were analyzed in a variety of different ways, all yielding the same conclusion that the ouabain treatment resulted in a significant and rapid loss of the visual-dependent behavioral response and then a gradual recovery. A repeated measures ANOVA analysis confirmed that the data set for the ouabain-treated fish was significantly different from the control fish data set ($p < 0.002$). Visual function in the control group varied only slightly over the time-course of the experiment (one-way ANOVA, $p = 0.95$), while the visual function of the experimental fish decreased to a minimum at 7 days after ouabain treatment (one-way ANOVA, $p < 0.0001$), and then gradually increased to approximate the control levels at the later time points. We performed a Tukey's *post hoc* multiple comparison test, comparing each experimental time point to pooled control data (Fig. 6), to determine the extent to which the ouabain treatment resulted in significant loss of vision, and whether this loss was followed by functional recovery. In this analysis, significant differences were indicated for all time points except for 98 days and beyond, suggesting an immediate loss of visual function, followed by recovery of visual function to match that of control fish within 98 days of treatment.

As a supplement to the escape response assay, the DLR was monitored daily in a separate set of fish that had been treated with ouabain in only one eye. Intraocular injection of 10 μM ouabain resulted in an abnormal body tilt within 24 h of treatment (Table 1). This abnormal body tilt was sustained for most fish throughout the postinjection survival time. We observed a return to a normal body position in 5 of the 11 fish that survived beyond 100 dpi (Table 1), consistent with successful regeneration of visual function for at least these four fish. We also

note that the remaining six fish in this group showed quite extensive iris overgrowth in the treated eyes, which may have precluded visual function even if the neural basis for vision had functionally regenerated (Table 1).

DISCUSSION

A Time-Course of Functional Regeneration of Whole Zebrafish Retina

Functional regeneration of zebrafish retina following intraocular injection of ouabain appears to occur in two distinct phases (Fig. 7). The first phase takes place over the initial 20 days of recovery, and consists of robust and rapid retinal histogenesis. The second phase takes place over the following 80 or more days and consists of RGC axon growth, pathfinding, and the return of visual function.

Zebrafish exposed to BrdU from 5 to 6 days after ouabain treatment incorporated BrdU into new retina cells, and the peak of retinal proliferation took place on or about 7 days after ouabain treatment. Some of the eyes examined 8 days after ouabain treatment contained retinal tissue with hints of an RGC layer. The transcription factor *ath5*, which is expressed just before the onset of retinal neurogenesis in the zebrafish embryo (Masai et al., 2000), and is required for RGC production (Kay et al., 2001), is expressed in regenerating retina at 6 and 8 days after ouabain treatment. These data suggest that initial neurogenesis and production of at least some RGCs takes place between 6 and 8 days following intraocular injection of the cytotoxin, similar to that seen in surgical and cell-selective lesion models in the zebrafish (Yurco and Cameron, 2005; Fimbel et al., 2007).

Within 12–14 days of exposure to ouabain, many of the treated eyes were found to contain retinas with three recognizable retinal layers, with intervening plexiform layers established. The patterns of expression of retina-specific markers such as islet-1 and *pax6* resembled the patterns for these markers in mature, undamaged retina (Figs. 3(J,K) and 4(B,C)]. These data indicate that the retinal cell types needed for retinal function are present and in the approximately correct histological positions within 2 weeks of retinal destruction by ouabain.

After the establishment of a histologically accurate retina at 2 weeks postinjection, there was a considerable delay before the statistically measurable return of visual function, at 98 days postinjection and beyond. We hypothesized that this delay may correspond to the time needed for newly-generated RGCs to grow axons, and for these axons to find their way to the ONH and beyond, for the establishment of functional connections, and for myelination of the optic nerve. The measurements of ONH diameter over time following ouabain treatment are consistent with this hypothesis. Although the ONH may have experienced some pathological changes at time points proximal to the ouabain treatment, from 20 to 210 days after ouabain injection, the ONHs steadily increased in size. Interestingly, the time that the size of the regenerating ONH reached/surpassed the size of control ONHs (between 85 and 120 days; Fig. 5), corresponded to the time at which recovery of visual function was observed (DLR, Table 1; escape response; Fig. 6). It is possible that this coincidence reflects a requirement for some threshold number of RGC axons to reach targets to support this behavior. In the goldfish, at least some regenerated ganglion cell axons reach the tectum within 16 days of a ouabain lesion, while the myelination of the optic nerve requires 28 days (Wolburg, 1981). However, rather tortuous and misrouted RGC axons were observed on the vitreal surface of the regenerating goldfish retina (Stuermer et al., 1985), suggesting that some RGC axons may not have access to the appropriate guidance cues or that the regenerated RGCs themselves lack intrinsic information for pathfinding within the eye. In the present study, over the time of regeneration, initially robust expression of the cell-surface, axonal adhesion marker neurolin (zn-8) steadily decreased to the nominally detectable amounts seen in undamaged adult retina. Neurolin expression in embryonic retina follows a similar temporal trajectory, with strong expression

following RGC neurogenesis, and reduced expression once initial connections were established with the optic tectum (Laessing and Stuermer, 1996). These data suggest that neurolin expression is not likely to be a limiting factor for the growth and targeting of axons of regenerated RGCs.

Multiple behavioral measures of functional recovery have now been used in two cyprinids, goldfish and zebrafish, to evaluate the return of vision following widespread retinal damage. In the goldfish, metabolic activity in the visually-deprived optic tectum begins to return 70–100 days after the ouabain treatment (Melzer and Powers, 2001), while the DLR recovers gradually over 50–210 days (Mensinger and Powers, 1999). Recovery of optokinetic nystagmus, a behavior that requires some degree of spatial resolution, has been documented at 99 days after ouabain treatment (Kästner and Wolburg, 1982). In the present study, we observed a return of a normal body position in a minor fraction of the treated fish by 100 dpi, and the complete recovery of the escape response, a behavior that requires spatial resolution, by 98 days or earlier, suggesting a time frame for visual recovery similar to that of goldfish. We note, however, that direct comparisons among these findings are not warranted. For example, our assessment of the DLR consisted of “normal” vs. “abnormal” as it was not possible to obtain actual measurements of degrees of tilt, as was possible with the more slowly-moving goldfish (Mensinger and Powers, 1999). In addition, the assays of visual function that require spatial resolution, the escape response (present study) and the optokinetic reflex (Kästner and Wolburg, 1982) measured either recovery-related changes in visual threshold, or the presence vs. the absence of visual function at a single light level, respectively. We were surprised that the functional recovery rate of the zebrafish was not faster than that of the larger goldfish, considering that regenerating ganglion cell axons have a shorter distance to traverse in the zebrafish, and considering that histological restoration of the retina occurs at a faster pace. For this reason we suspect that RGC axon pathfinding may be a limiting factor for functional regeneration in the zebrafish. The correlation of ONH size with the time of behavioral recovery is consistent with this hypothesis, and further suggests that pathfinding within the eye, to the ONH, may be the restrictive process.

Does Regeneration Recapitulate Development?

A large body of evidence has collectively indicated that the process of retinal neurogenesis in teleost fish may represent a re-initiation and subsequent deployment of the embryonic retinal neurogenesis program (Stenkamp, 2007; Hitchcock et al., 2004). Much of the evidence has come from the study of expression of individual genes during embryonic retinal neurogenesis and during retinal regeneration. For example, early in the regeneration process, within days of chemical or mechanical damage, cells express genes typical of retinal progenitors, including *pax6* (Hitchcock et al., 1996), *vsx-1* (Levine et al., 1994), *Notch-3* (Sullivan et al., 1997), and *n-cadherin* (Liu et al., 2002), and a transgene reporting expression of *atoh-7* (Fimbel et al., 2007). Ours is the first study to evaluate expression of multiple genes involved in neurogenesis and retinal cell differentiation, and to evaluate the relative spatiotemporal patterns of expression of these genes during whole-tissue retinal regeneration. We selected genes that are involved in the neurogenesis of RGCs, because these are the physiological output cells of the eye, and because the deployment of an accurate genetic program for RGC differentiation may be required for these cells to grow axons that establish functional connections (Mu and Klein, 2004). We find that, during retinal regeneration, the relative spatiotemporal patterns of expression of *ath5*, *pax6*, islet-1, Hu protein, and neurolin, mimicked the corresponding relative spatiotemporal patterns for these markers during embryonic retinal neurogenesis. In regenerating retina, *ath5* was expressed early and transiently, as is the case for embryonic retinal neurogenesis (Kay et al., 2001). *Pax6* was also expressed early in regeneration, and initially throughout an apparently neuroepithelial layer, before becoming restricted to the RGC layer and the INL, similar to the situation for developing embryonic retina (Puschel et al.,

1992; Hitchcock et al., 1996; Nornes et al., 1998). Expression of both islet-1 and Hu protein was apparent when RGCs were first recognizable during retinal regeneration, and this is also true of embryonic islet-1 and Hu protein expression (Korzh et al., 1998). The expression of the cell adhesion molecule neurolin, was delayed relative to these other markers during retinal regeneration, and its expression then declined over time. Similarly, zebrafish embryonic retinas express neurolin at 28 h post-fertilization (hpf) (Laessing and Stuermer, 1996), as compared to the expression of *ath5* [25 hpf; (Masai et al., 2000)], and expression of neurolin is most robust embryonically and declines thereafter (Laessing and Stuermer, 1996). Together, these findings indicate that the developmental genetic cascade of embryonic RGC neurogenesis is recapitulated during RGC regeneration.

There are, however, some potentially important differences in RGC regeneration as compared to embryonic RGC neurogenesis. Some of the RGC markers we tested in regenerating retina failed to label retinal tissue at any time of the regenerative process, even while they successfully labeled embryonic RGCs. The RGC markers *Brn3b*, *fgf8*, and *shh*, label embryonic RGCs beginning at or before 40 hpf (DeCarvalho et al., 2004), 34 hpf (Stenkamp and Frey, 2003), and 28 hpf (Neumann and Nuesslein-Volhard, 2000), respectively. However, expression of these genes was undetectable in undamaged, or in regenerating retina at any time point tested, suggesting that these genes may not be re-expressed during retinal regeneration at levels detectable by *in situ* hybridization. In support of this interpretation are recent results from a gene profiling study of intact zebrafish retina, and of zebrafish retina following a surgical lesion (Cameron et al., 2005). In this study (series accession number GSE3303, and Cameron, personal communication), the level of *pax6* mRNA expression in undamaged zebrafish retina (Affymetrix signal = 3400 units), which is detectable by *in situ*, is far greater than the levels of *Brn3b* (Affymetrix signal = 450 units), *fgf8* (Affymetrix signal = 130 units), or *shh* (Affymetrix signal = 160 units). Furthermore, expression of these genes was not significantly upregulated at 2 or 14 days following a surgical lesion (Cameron, personal communication). It is therefore possible that, with respect to these three genes, regeneration may *not* recapitulate development. While it is important that these results be verified by a quantitative method, and following ouabain treatment, it is also tempting to speculate that they may represent errors in RGC development during regeneration. In turn, these errors may lead to RGC axon pathfinding difficulties or other irregularities such as the excess production of cells in the RGC layer. In support of this hypothesis, Brn3b is known to regulate *shh* expression (Mu et al., 2004), which in turn is known to regulate RGC number (Zhang and Yang, 2001). Furthermore, although Brn3b is not necessary for RGC neurogenesis, it is needed to promote the mature RGC phenotype (Gan et al., 1999), and RGCs in mice lacking Brn3b display axon pathfinding defects (Wang et al., 2002).

There is evidence that retinal injuries result in the re-establishment of microenvironmental features that resemble the stem cell environments of embryonic retina and the CGZ (Raymond et al., 2006). In turn, these “stem cell niches” support retinal neurogenesis from Müller glia that re-enter the cell cycle and become pluripotent (Bernardos et al., 2007). The present study suggests that, following widespread retinal damage, these stem cell niches may not contain information sufficient to support a complete recapitulation of the developmental process.

Whole-Retina Regeneration: Challenges as well as Opportunities

A goal of the present study was to assess both the capacities and the limitations of whole tissue retinal regeneration in teleosts so that these issues are recognized and addressed in future applications in humans. One consistent finding for those studying retinal regeneration in teleost fish, is that extraretinal tissues of the eye appear to be influenced by the process. It is typical to see gross morphological defects in the iris and lens that may impair the recovery of visual function. Another consistent finding is that the newly-generated retina shows lamination

defects, with cell bodies present in ectopic locations, predominantly within the inner plexiform layer. Finally, as recovery time progresses, the density of cells in or associated with the RGC layer expands beyond the density of cells in the RGC layers of native retina. We suspect that these additional cells may be RGCs because prolonged recovery time is also associated with excessive growth of the ONH. These excess cells may represent overproduction of RGCs and/or a failure to prune RGC numbers by apoptosis, as occurs during embryonic development (Biehlmaier et al., 2001). This finding is consistent with an earlier study that showed high RGC densities in regenerated retina following a surgical lesion (Cameron and Carney, 2000). Therefore, while the regenerative process is quite capable of robust proliferation and neurogenesis sufficient to repopulate the eye with functional retinal cells, it may not be capable of recognizing when the process is complete. Any application of retinal regenerative therapy in humans may therefore need to address the need to stop regeneration as well as to start it. A final challenge for whole tissue retinal regeneration is the requirement for RGC axons to navigate to their appropriate targets. Observed behavioral recovery indicates that the axons of at least some regenerated RGCs can accomplish this task, and our measurements of the ONH indicate that a large number of RGC axons do successfully navigate to the exterior of the eye. However, adjustments of the retinal and optic nerve environment may be needed to optimize this process.

Acknowledgements

Authors thank Drs. Jim Fadool (Florida State U.) and Steven Wilson (King's College, London) for providing cDNAs, Dr. David Cameron (SUNY Upstate Medical U.) for providing quantitative gene expression (Affymetrix) data, and Ms. Ruth Frey (U. Idaho) for technical assistance.

This work was supported by a Fight For Sight summer research fellowship (DEM).

Contract grant sponsor: The Glaucoma Foundation.

Contract grant sponsor: NIH; contract grant numbers: R01 EY012146, P20 RR016454.

Contract grant sponsor: NSF (REU Site: Summer Computational Neuroscience & Technology Research Experience for Undergraduates); contract grant number: 0243885.

Contract grant sponsor: Department of Biological Sciences, University of Idaho and the Center for Zebrafish Research at the University of Notre Dame.

References

Ahmad I, Tang L, Pham H. Identification of neural progenitors in the adult mammalian eye. Biochem Biophys Res Commun 2000;270:517–521. [PubMed: 10753656]

Barthel LK, Raymond PA. Improved method for obtaining 3-micron cryosections for immunocytochemistry. J Histochem Cytochem 1990;38:1383–1388. [PubMed: 2201738]

Barthel LK, Raymond PA. Subcellular localization of α-tubulin and opsin mRNA in the goldfish retina using digoxigenin-labeled cRNA probes detected by alkaline phosphatase and HRP histochemistry. J Neurosci Methods 1993;50:145–152. [PubMed: 8107495]

Bernardos RL, Barthel LK, Meyer JR, Raymond PA. Late-stage neuronal progenitors in the retina are radial Muller glia that function as retinal stem cells. J Neurosci 2007;27:7028–7040. [PubMed: 17596452]

Biehlmaier O, Nuehauss SC, Kohler K. Onset and time course of apoptosis in the developing zebrafish retina. Cell Tissue Res 2001;306:199–207. [PubMed: 11702231]

Braisted JE, Essman TF, Raymond PA. Selective regeneration of photoreceptors in goldfish retina. Development 1994;120:2409–2419. [PubMed: 7956821]

Cameron DA. Cellular proliferation and neurogenesis in the injured retina of adult zebrafish. Vis Neurosci 2000;17:789–797. [PubMed: 11153658]

Cameron DA, Carney LH. Cell mosaic patterns in the native and regenerated inner retina of zebrafish: Implications for retinal assembly. J Comp Neurol 2000;416:356–367. [PubMed: 10602094]

Cameron DA, Gentile KL, Middleton FA, Yurco P. Gene expression profiles of intact and regenerating zebrafish retina. Mol Vis 2005;11:775–791. [PubMed: 16205622]

DeCarvalho AC, Cappendijk SL, Fadool JM. Developmental expression of the POU domain transcription factor Brn-3b (Pou4f2) in the lateral line and visual system of zebrafish. Dev Dyn 2004;229:869–876. [PubMed: 15042710]

Eichler VB, Taylor PW. A new metachromatic stain technique for paraffin-embedded neural tissue using thionin. J Microsc 1976;108:97–99. [PubMed: 64611]

Fashena D, Westerfield M. Secondary motoneuron axons localize DM-GRASP on their fasciculated segments. J Comp Neurol 1999;406:415–424. [PubMed: 10102505]

Fausett BV, Goldman D. A role for α1 tubulin-expressing Muller glia in regeneration of the injured zebrafish retina. J Neurosci 2006;26:6303–6313. [PubMed: 16763038]

Fimbel SM, Montgomery JE, Burket CT, Hyde DR. Regeneration of inner retinal neurons after intravitreal injection of ouabain in zebrafish. J Neurosci 2007;27:1712–1724. [PubMed: 17301179]

Fischer AJ, Reh TA. Muller glia are a potential source of neural regeneration in the postnatal chicken retina. Nat Neurosci 2001;4:247–252. [PubMed: 11224540]

Galli-Resta L, Resta G, Tan SS, Reese BE. Mosaics of islet-1-expressing amacrine cells assembled by short-range cellular interactions. J Neurosci 1997;17:7831–7838. [PubMed: 9315903]

Gan L, Wang SW, Huang Z, Klein WH. POU domain factor Brn-3b is essential for retinal ganglion cell differentiation and survival but not for initial cell fate specification. Dev Biol 1999;210:469–480. [PubMed: 10357904]

Hitchcock P, Ochocinska M, Sieh A, Otteson D. Persistent and injury-induced neurogenesis in the vertebrate retina. Prog Retin Eye Res 2004;23:183–194. [PubMed: 15094130]

Hitchcock PF, Lindsey Myhr KJ, Easter SS Jr, Mangione-Smith R, Jones DD. Local regeneration in the retina of the goldfish. J Neurobiol 1992;23:187–203. [PubMed: 1527527]

Hitchcock PF, Macdonald RE, VanDeRyt JT, Wilson SW. Antibodies against Pax6 immunostain amacrine and ganglion cells and neuronal progenitors, but not rod precursors, in the normal and regenerating retina of the goldfish. J Neurobiol 1996;29:399–413. [PubMed: 8907167]

Hu M, Easter SS. Retinal neurogenesis: The formation of the initial central patch of postmitotic cells. Dev Biol 1999;207:309–321. [PubMed: 10068465]

Johns PR, Fernald RD. Genesis of rods in teleost fish retina. Nature 1981;293:141–142. [PubMed: 7266666]

Julian D, Ennis K, Korenbrot JI. Birth and fate of proliferative cells in the inner nuclear layer of the mature fish retina. J Comp Neurol 1998;394:271–282. [PubMed: 9579393]

Kassen SC, Ramanan V, Montgomery JE, Burket CT, Liu CG, Vihtelic TS, Hyde DR. Time course analysis of gene expression during light-induced photoreceptor cell death and regeneration in *albino* zebrafish. Dev Neurobiol 2007;67:1009–1031. [PubMed: 17565703]

Kästner R, Wolburg H. Functional regeneration of the visual system in teleosts. Comparative investigations after optic nerve crush and damage of the retina. Z Naturforsch 1982;37:1274–1280.

Kay JN, Finger-Baier KC, Roeser T, Staub W, Baier H. Retinal ganglion cell genesis requires lakritz, a Zebrafish atonal Homolog. Neuron 2001;30:725–736. [PubMed: 11430806]

Kim CH, Ueshima E, Muraoka O, Tanaka H, Yeo SY, Huh TL, Miki N. Zebrafish elav/HuC homologue as a very early neuronal marker. Neurosci Lett 1996;216:109–112. [PubMed: 8904795]

Korzh V, Sleptsova I, Liao J, He J, Gong Z. Expression of zebrafish bHLH genes ngn1 and nrd defines distinct stages of neural differentiation. Dev Dyn 1998;213:92–104. [PubMed: 9733104]

Laessing U, Stuermer CA. Spatiotemporal pattern of retinal ganglion cell differentiation revealed by the expression of neurolin in embryonic zebrafish. J Neurobiol 1996;29:65–74. [PubMed: 8748372]

Levine EM, Hitchcock PF, Glasgow E, Schechter N. Restricted expression of a new paired-class homeobox gene in normal and regenerating adult goldfish retina. J Comp Neurol 1994;348:596–606. [PubMed: 7836564]

Li L, Dowling JE. A dominant form of inherited retinal degeneration caused by a non-photoreceptor cell-specific mutation. Proc Natl Acad Sci USA 1997;94:11645–11650. [PubMed: 9326664]

Li L, Dowling JE. Zebrafish visual sensitivity is regulated by a circadian clock. Vis Neurosci 1998;15:851–857. [PubMed: 9764527]

Liu Q, Londraville RL, Azodi E, Babb SG, Chiappini-Williamson C, Marrs JA, Raymond PA. Up-regulation of cadherin-2 and cadherin-4 in regenerating visual structures of adult zebrafish. Exp Neurol 2002;177:396–406. [PubMed: 12429186]

Lambardo F. Time course and localization of mitoses during the regeneration of the retina of an adult telost-published in Italian. Accademia Lincei-Reniconti Scienze Fisicali Matematiche e Naturale 1972;53:323–327.Series 8

Maier W, Wolburg H. Regeneration of the goldfish retina after exposure to different doses of ouabain. Cell Tissue Res 1979;202:99–118. [PubMed: 509506]

Marcus RC, Delaney CL, Easter SS Jr. Neurogenesis in the visual system of embryonic and adult zebrafish (*Danio rerio*). Vis Neurosci 1999;16:417–424. [PubMed: 10349963]

Martinez-Morales JR, Del Bene F, Nica G, Hammerschmidt M, Bovolenta P, Wittbrodt J. Differentiation of the vertebrate retina is coordinated by an FGF signaling center. Dev Cell 2005;8:565–574. [PubMed: 15809038]

Masai I, Stemple DL, Okamoto H, Wilson SW. Midline signals regulate retinal neurogenesis in zebrafish. Neuron 2000;27:251–263. [PubMed: 10985346]

Melzer P, Powers MK. Metabolic activity in optic tectum during regeneration of retina in adult goldfish. Vis Neurosci 2001;18:599–604. [PubMed: 11829305]

Mensinger AF, Powers MK. Visual function in regenerating teleost retina following cytotoxic lesioning. Vis Neurosci 1999;16:241–251. [PubMed: 10367959]

Mu X, Beremand PD, Zhao S, Pershad R, Sun H, Scarpa A, Liang S, Thomas TL, Klein WH. Discrete gene sets depend on POU domain transcription factor Brn3b/Brn-3.2/POU4f2 for their expression in the mouse embryonic retina. Development 2004;131:1197–1210. [PubMed: 14973295]

Mu X, Klein WH. A gene regulatory hierarchy for retinal ganglion cell specification and differentiation. Semin Cell Dev Biol 2004;15:115–123. [PubMed: 15036214]

Neumann CJ, Nuesslein-Volhard C. Patterning of the zebrafish retina by a wave of sonic hedgehog activity. Science 2000;289:2137–2139. [PubMed: 11000118]

Nornes S, Clarkson M, Mikkola I, Pedersen M, Bardsley A, Martinez JP, Krauss S, Johansen T. Zebrafish contains two pax6 genes involved in eye development. Mech Dev 1998;77:185–196. [PubMed: 9831649]

Ott H, Diekmann H, Stuermer CA, Bastmeyer M. Function of neurolin (DM-GRASP/SC-1) in guidance of motor axons during zebrafish development. Dev Biol 2001;235:86–97. [PubMed: 11412029]

Otteson DC, D'Costa AR, Hitchcock PF. Putative stem cells and the lineage of rod photoreceptors in the mature retina of the goldfish. Dev Biol 2001;232:62–76. [PubMed: 11254348]

Puschel AW, Gruss P, Westerfield M. Sequence and expression pattern of pax-6 are highly conserved between zebrafish and mice. Development 1992;114:643–651. [PubMed: 1352238]

Raymond PA. Cytodifferentiation of photoreceptors in larval goldfish: Delayed maturation of rods. J Comp Neurol 1985;236:90–105. [PubMed: 4056092]

Raymond PA, Barthel LK, Bernardos RL, Perkowski JJ. Molecular characterization of retinal stem cells and their niches in adult zebrafish. BMC Dev Biol 2006;26:6–36.

Raymond PA, Easter SS Jr. Postembryonic growth of the optic tectum in goldfish. I. Location of germinal cells and numbers of neurons produced. J Neurosci 1983;3:1077–1091. [PubMed: 6842282]

Raymond PA, Reifler MJ, Rivlin PK. Regeneration of goldfish retina: Rod precursors are a likely source of regenerated cells. J Neurobiol 1988;19:431–463. [PubMed: 3392530]

Raymond PA, Rivlin PK. Germinal cells in the goldfish retina that produce rod photoreceptors. Dev Biol 1987;122:120–138. [PubMed: 3596007]

Silver PH. Photopic spectral sensitivity of the neon tetra (*Paracheirodon innesi* (Myers)) found by the use of a dorsal light reaction. Vis Res 1974;14:329–334. [PubMed: 4830684]

Stenkamp DL. Neurogenesis in the Fish Retina. Int Rev Cytol 2007;259:173–224. [PubMed: 17425942]

Stenkamp DL, Frey RA. Extraretinal and retinal hedgehog signaling sequentially regulate retinal differentiation in zebrafish. Dev Biol 2003;258:349–363. [PubMed: 12798293]

Stenkamp DL, Powers MK, Carney LH, Cameron DA. Evidence for two distinct mechanisms of neurogenesis and cellular pattern formation in regenerated goldfish retinas. J Comp Neurol 2001;431:363–381. [PubMed: 11223808]

Stuermer CA, Niepenberg A, Wolburg H. Aberrant axonal paths in regenerated goldfish retina and tectum opticum following intraocular injection of ouabain. Neurosci Lett 1985;58:333–338. [PubMed: 4047493]

Sullivan SA, Barthel LK, Largent BL, Raymond PA. A goldfish notch-3 homologue is expressed in neurogenic regions of embryonic, adult, and regenerating brain and retina. Dev Genet 1997;20:208–223. [PubMed: 9216061]

Tropepe V, Coles BL, Chiasson BJ, Horsford DJ, Elia AJ, McInnes RR, van der Kooy D. Retinal stem cells in the adult mammalian eye. Science 2000;287:2032–2036. [PubMed: 10720333]

Vihtelic TS, Hyde DR. Light-induced rod and cone cell death and regeneration in the adult albino zebrafish (*Danio rerio*) retina. J Neurobiol 2000;44:289–307. [PubMed: 10942883]

Wang SW, Mu X, Bowers WJ, Kim DS, Plas DJ, Crair MC, Federoff HJ, et al. Brn3b/Brn3c double knockout mice reveal an unsuspected role for Brn3c in retinal ganglion cell axon outgrowth. Development 2002;129:467–477. [PubMed: 11807038]

Westerfield, M. The Zebrafish Book: A Guide for the Laboratory Use of Zebrafish (*Danio rerio*). 4. Eugene, OR: University of Oregon; 2000.

Wolburg H. Time- and dose-dependent influence of ouabain on the ultrastructure of optic neurones. Cell Tissue Res 1975;164:503–517. [PubMed: 1203964]

Wolburg H. Axonal transport, degeneration and regeneration in the visual system of the goldfish. Adv Anat Embryol Cell Biol 1981;67:1–94. [PubMed: 6164262]

Wu DM, Schneiderman T, Burgett J, Gokhale P, Barthel L, Raymond PA. Cones regenerate from retinal stem cells sequestered in the inner nuclear layer of adult goldfish retina. Invest Ophthalmol Vis Sci 2001;42:2115–2124. [PubMed: 11481280]

Yurco P, Cameron DA. Responses of Muller glia to retinal injury in adult zebrafish. Vis Res 2005;45:991–1002. [PubMed: 15695184]

Zhang XM, Yang XJ. Regulation of retinal ganglion cell production by sonic hedgehog. Development 2001;128:943–957. [PubMed: 11222148]

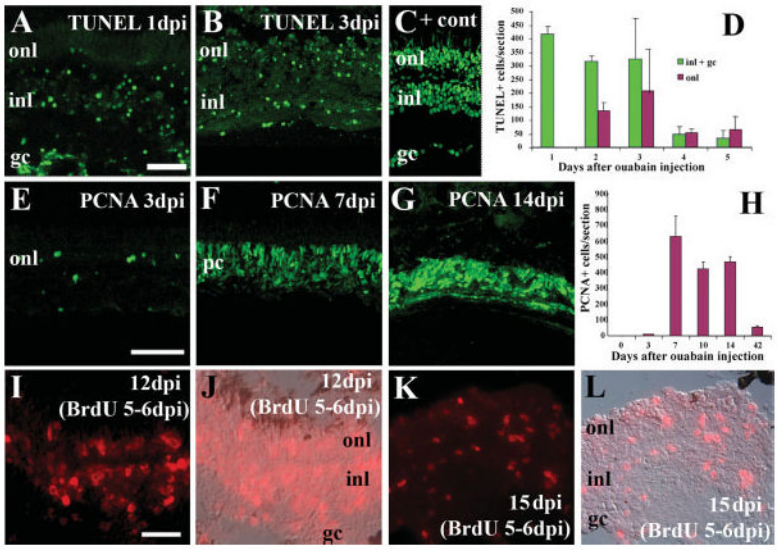

Figure 1.

Widespread retinal cell death is followed by retinal cell proliferation to regenerate all retinal layers in response to intraocular injection of 10 μm ouabain. A, B: TUNEL-positive cells (green fluorescence) are present at 1 (A) and 3 (B) dpi. Panel C: shows a positive control section (+ cont) that was treated with TACS-nuclease. D: TUNEL labeling was quantified according to days after ouabain treatment and laminar position of labeled cells. Columns represent means ± SD. (n = 6 retinas for each time). E–G: Small numbers of PCNA+ cells (green fluorescence) are found at 3 dpi (E), but are widespread at 7 (F) and 10 (G) dpi. H. PCNA labeling was quantified according to days after ouabain treatment. Columns represent means ± S.D. (n = 6 retinas for each time). I–L: BrdU incorporation (red fluorescence) indicates all layers of retinal tissue were generated following an intraocular injection of ouabain. Fish were systemically exposed to 5 m*M* BrdU for 48 h, beginning 5 days after ouabain treatment (see Methods), and sacrificed 12 days (I,J) and 15 days (K,L) after ouabain treatment. Panels I and K: depict BrdU fluorescence only; panels J and L: show overlays with a Nomarski image. Scale bar in A (applies to A–C) = 50 μm; bar in E (applies to E–G) = 75 μm; dpi, bar in I (applies to I–L) = 25 μm; dpi days postinjection; onl, outer nuclear layer; inl, inner nuclear layer; gc, ganglion cell layer; pc, progenitor cells.

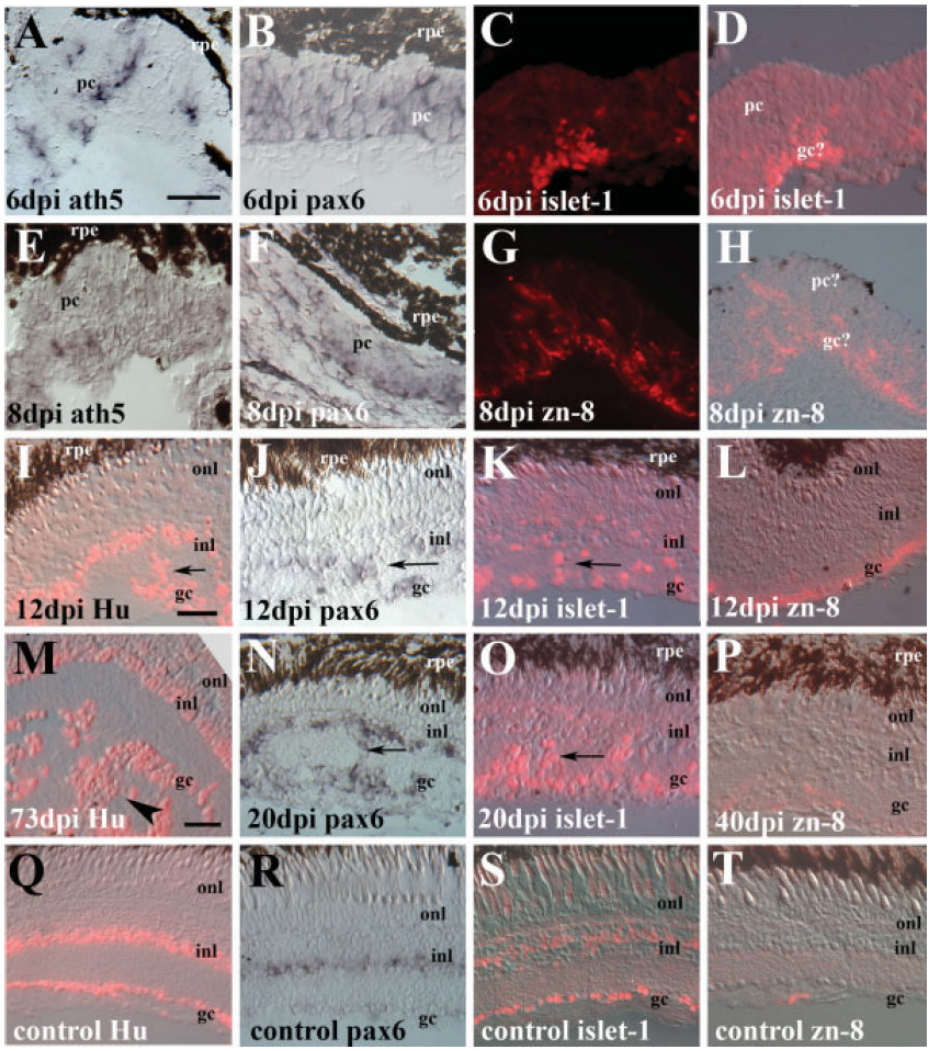

Figure 2.

Gene expression in regenerating retina obtained at six (A–D), eight (E–H), 12 (I–L), 20 (N,O), 40 (P), and 73 days (M) following intraocular injection of 10 μM ouabain, as compared to gene expression in undamaged control retinas (Q–T). Tissue was hybridized with cRNA probes corresponding to *ath5* (A, E) or *pax6* (B, F, J, N, and R), or was processed for indirect immunofluorescence with antibodies for islet-1 (C, D, K, O, and S), zn-8/neurolin (G, H, L, P, and T), or Hu protein (I, M, and Q). Both fluorescence-only images (C,G), and fluorescence merged with Nomarski images (D,H) are shown in cases of weaker labeling. Scale bar in A (applies to A–H) = 20 μm; scale bar in I (applies to I–L) = 20 μm; scale bar in M (applies to M–T) = 20 μm. All images are oriented with the vitreal surface of the retina on the bottom; dpi, days post-injection; rpe, retinal pigmented epithelium; pc, progenitor cells; gc, ganglion cell layer; inl, inner nuclear layer; onl, outer nuclear layer. Arrows depict regions of laminar fusion within the inner plexiform layer.

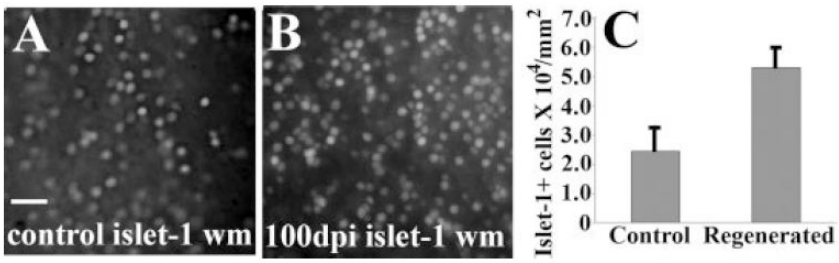

Figure 3.

Density/topography of islet-1+ cells in undamaged (A) and regenerating retina obtained at over 100 days (B) following intraocular injection of 10 μM ouabain. Panels A and B are views of whole-mounted retinas, ganglion cell side-up, with a focal plane corresponding to the region of the GC layer having the highest cell density. Scale bar (applies to A and B) = 20 μm; dpi, days postinjection; wm, whole mount. C. Average (± S.D.) density of islet-1-positive cells in representative, optically coplanar regions of whole mounted native (control) and regenerated retina.

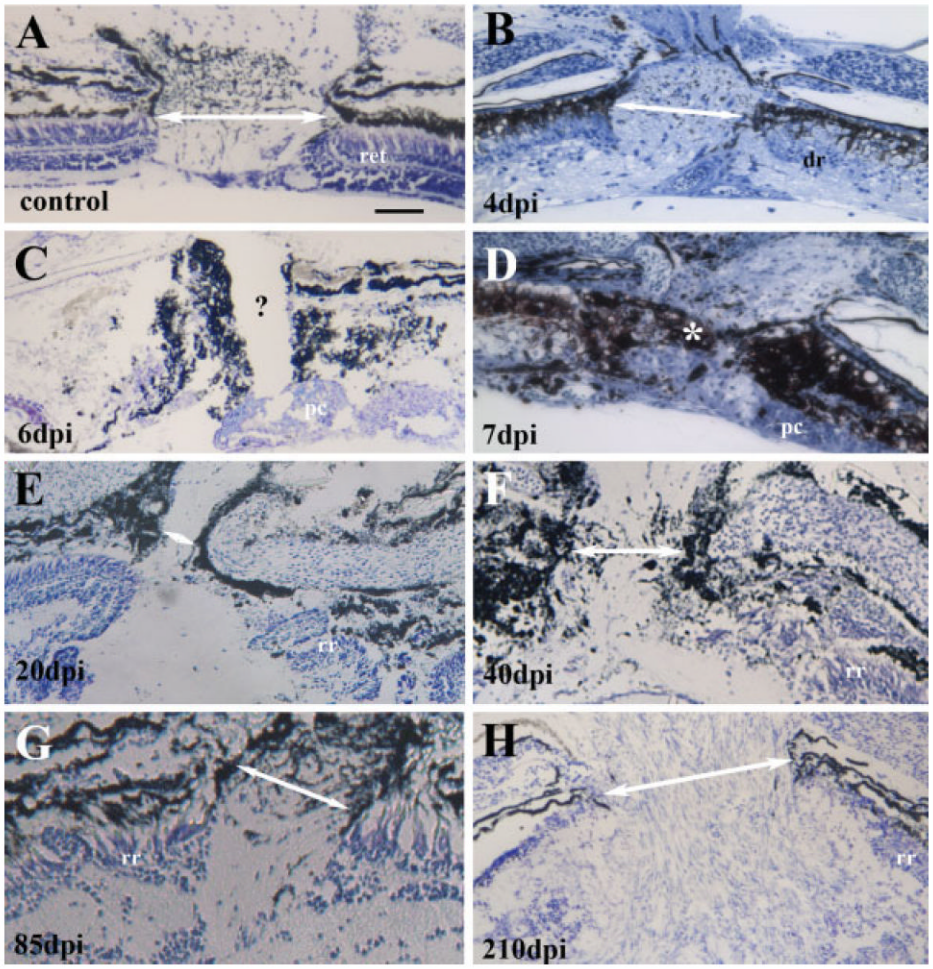

Figure 4.

Optic nerve head morphology in undamaged (A) and regenerating retina obtained at 4 (B), 6 (C), 7 (D), 20 (E), 40 (F), 85 (G), and 210 days (H) following intraocular injection of 10 μM ouabain. Tissue was stained with thionin (A, C, and E–H) or methylene blue/azure II (B and D); image color balance was changed in some cases for color plate uniformity. Optic nerve head measurements are provided in Figure 5. White arrows in each panel indicate distance measured as optic nerve head diameter. Question mark in panel C shows probable optic nerve head region, lacking axons, and therefore scored as a diameter of zero. White asterisk in panel D indicates pigmented material apparently blocking the passage of axons; optic nerve head diameter in this case was also scored as zero. Scale bar (applies to all) = 50 μm; dpi, days postinjection; ret, retina; dr, degenerating retina; pc, progenitor cells; rr, regenerating retina.

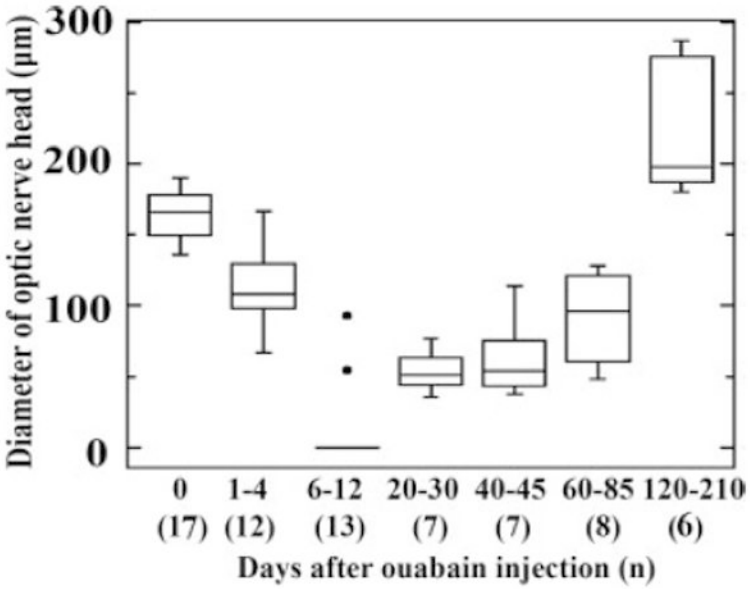

Figure 5.

Optic nerve head diameter as a function of time following intraocular injection of 10 μM ouabain. In this boxplot, boxes delineate the upper and lower quartiles, and whiskers indicate the range of values for each time point. The horizontal lines within each box indicate the means. The “0 days” time point includes data collected from contralateral control eyes obtained at several times after ouabain treatment. At 6–12 days, the median is zero, and the significant outliers are represented by filled circles. A measurement of zero indicates no axons were seen to pass from within the eye to the exterior of the eye.

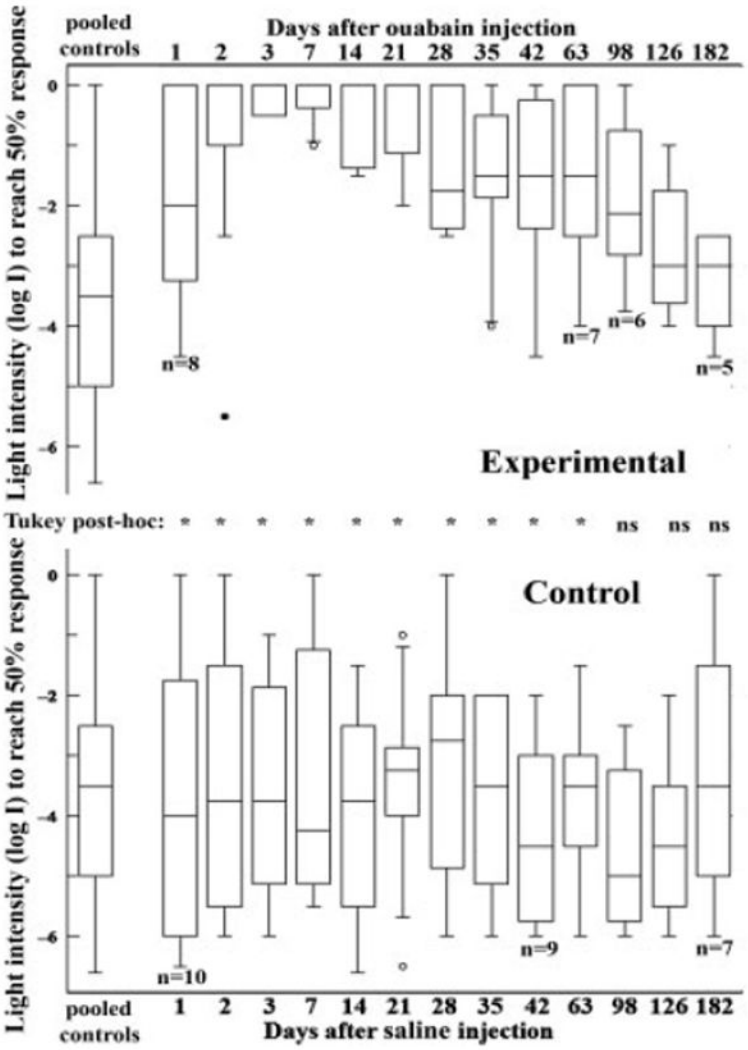

Figure 6.

Visual sensitivities of (A) 10 μM ouabain-treated (n = 8 initially) and (B) control (n = 10 initially) zebrafish as assayed by the escape response. In this experiment, the absolute visual threshold of a fish exhibiting an escape response at a given light level (log I = 0 corresponds to ambient light or 4.25×10^{-3} $\mu W/cm^2$) is determined by quantifying the number of escapes to a moving visual stimulus. In both A and B, the leftmost boxplot describes pooled data for all control measurements; remaining boxplots are plotted according to time of assay following injection of the ouabain-treated animals. Boxes delineate the upper and lower quartiles, and whiskers indicate the range of values for each time point (outliers are represented by open circles and significant outliers by filled circles). Statistical analysis (inset between A and B) demonstrated loss and recovery of visual function in the ouabain-treated zebrafish. A Tukey *post hoc* multiple comparisons test revealed significant differences (*) in visual threshold in ouabain-treated vs. pooled controls at all time points except those at 98 days and beyond. ns, not significant.

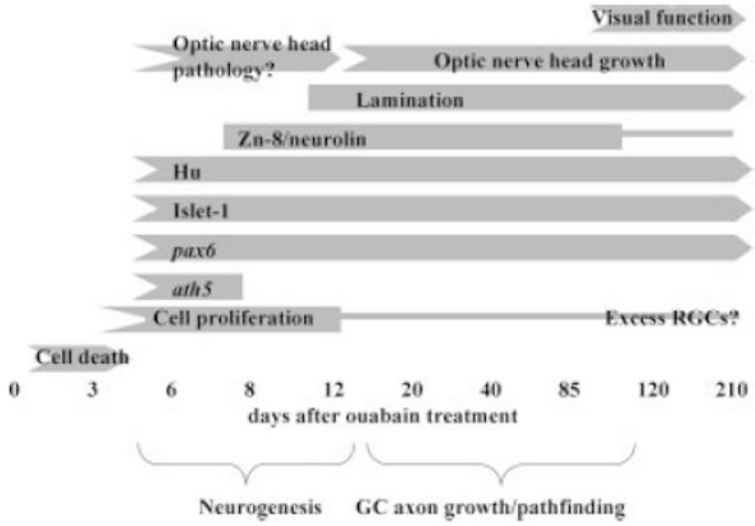

Figure 7.
Summary of the process of retinal regeneration in zebrafish following intraocular injection of 10 μM ouabain.

Table 1

Ocular Gross Anatomy and Dorsal Light Reflex Following Intraocular Injection of 10 μM Ouabain

	Postmortem Analysis of Ocular Gross Anatomy						Analysis of Live Fish	
Days Postinjection	**Abnormal Eye Morphology**	**(+/*n*)**	**Abnormal Iris**	**(+/*n*)**	**Abnormal Lens**	**(+/*n*)**	**Abnormal DLR**	**(+/*n*)**
0							–	(0/38)
1							+	(38/38)
6	+	(1/6)	+	(1/6)	+	(0/6)	+	(38/38)
8	+	(2/4)	+	(2/4)	+	(0/4)	+	(32/32)
12	+	(2/6)	+	(3/6)	+	(0/6)	+	(28/28)
20	+	(2/5)	+	(2/5)	+	(0/5)	+	(22/22)
40–90	+	(4/6)	+	(4/6)	+	(1/6)	+	(17/17)
100+	+	(6/11)	+	(8/11)	+	(2/11)	+	(6/11)

Table 2

Retinal Gene Expression Following Intraocular Injection of 10 μM Ouabain

	In Situ Hybridization										Immunocytochemistry					
Days Postinjection	***Ath5***	**(+/*n*)**	***Pax6***	**(+/*n*)**	***Brn3b***	**(+/*n*)**	***Fgf8***	**(+/*n*)**	***Shh***	**(+/*n*)**	**Islet-1**	**(+/*n*)**	**Hu**	**(+/*n*)**	**Zn-8**	**(+/*n*)**
0	−	(0/5)	+	(4/4)	−	(0/5)	−	(0/5)	−	(0/5)	+	(3/3)	+	(5/5)	−	(0/8)
6	+	(4/4)	+	(3/3)	−	(0/4)	−	(0/4)	−	(0/4)	+	(1/1)	+	(3/3)	−	(0/3)
8	+	(3/5)	+	(2/2)	−	(0/4)	−	(0/4)	−	(0/4)	+	(4/4)	+	(2/2)	+	(3/5)
12	−	(0/2)	+	(2/2)	−	(0/3)	−	(0/3)	−	(0/3)	+	(2/2)	+	(2/2)	+	(4/4)
20	−	(0/2)	+	(2/2)	−	(0/2)	−	(0/2)	−	(0/2)	+	(2/2)	+	(2/2)	+	(2/2)
40–90	n.d.		n.d.		−	(0/1)	−	(0/1)	−	(0/1)	+	(2/2)	+	(4/4)	+	(2/5)
Embryonic retina (36 hpf)	+		+		+		+		+		+		+		+	